Am J Physiol Renal Physiol 310: F342–F350, 2016.
First published December 9, 2015; doi:10.1152/ajprenal.00204.2015.

HL156A, a novel AMP-activated protein kinase activator, is protective against peritoneal fibrosis in an in vivo and in vitro model of peritoneal fibrosis

Kyung Don Ju,[1] Hyo Jin Kim,[2] Bodokhsuren Tsogbadrakh,[1] Jinho Lee,[1] Hyunjin Ryu,[2] Eun Jin Cho,[2] Young-Hwan Hwang,[4] Kiwon Kim,[5] Jaeseok Yang,[2,3] Curie Ahn,[2,3] and Kook-Hwan Oh[2]

[1]*Institute of Biomedical Research, Seoul National University Hospital, Seoul, Korea;* [2]*Department of Internal Medicine, Seoul National University Hospital, Seoul, Korea;* [3]*Institute of Transplantation Research, Seoul National University Hospital, Seoul, Korea;* [4]*Department of Internal Medicine, Eulji University, Seoul, Korea; and* [5]*Nephrology Clinic, National Cancer Center, Goyang, Korea*

Submitted 11 May 2015; accepted in final form 3 December 2015

Ju KD, Kim HJ, Tsogbadrakh B, Lee J, Ryu H, Cho EJ, Hwang YH, Kim KW, Yang J, Ahn C, Oh KH. HL156A, a novel AMP-activated protein kinase activator, is protective against peritoneal fibrosis in an in vivo and in vitro model of peritoneal fibrosis. *Am J Physiol Renal Physiol* 310: F342–F350, 2016. First published December 9, 2015; doi:10.1152/ajprenal.00204.2015.—HL156A is a novel AMP-activated protein kinase (AMPK) activator. We aimed to investigate the protective mechanism of HL156A against peritoneal fibrosis (PF) in in vivo and in vitro models. The rat PF model was induced by daily intraperitoneally injection of chlorhexidine (CHX) solution containing 0.1% CHX gluconate and 15% ethanol for 4 wk. The rats in the treatment group were treated with HL156A (1 $mg \cdot kg^{-1} \cdot day^{-1}$). Control rats were injected with vehicle alone. In vitro, cultured rat peritoneal mesothelial cells (RPMCs) were treated with either high glucose (HG; 50 mM), normal glucose (NG; 5 mM), NG+HL156A, or HG+HL156A. HL156A in supplemented rats ameliorated peritoneal calcification, cocoon formation, bowel obstruction, and PF. Immunohistochemistry showed reduced fibronectin accumulation in the peritoneum of HL156A-treated rats compared with those injected with CHX alone. HL156A treatment of RPMCs inhibited HG-induced myofibroblast transdifferentiation and markers of epithelial-mesenchymal transition (EMT). Moreover, HL156A ameliorated HG-induced transforming growth factor-β1, Smad3, Snail, and fibronectin expression in the RPMCs via AMPK upregulation. These results suggest that HL156A exhibits a protective effect in PF progression. Further research is warranted to seek the therapeutic potential of HL156A as an antifibrotic agent in peritoneal dialysis patients.

peritoneal fibrosis; HL156A; AMP kinase; epithelial-mesenchymal transition (EMT); fibronectin

PERITONEAL FIBROSIS (PF) IS one of the most serious complication of peritoneal dialysis (PD) which limits the effectiveness of PD as a long-term replacement therapy (13, 40). Extended exposures of the peritoneal membrane to a dialysis solution including supraphysiologically high glucose (HG) or to repeated peritonitis episode have been suggested to be contributing factors to the development of PF. PF is associated with the epithelial-mesenchymal transition (EMT) of peritoneal mesothelial cells, resulting in their transdifferentiation into myofibroblasts, contributing to the accumulation of extracellular matrix (ECM) molecules (1, 2, 8, 25, 29, 35). During the EMT process, epithelial cells mainly disrupt their adhesion capacity due to the decrease in E-cadherin and the cytoskeleton rearrangement, leading to the upregulation of α-smooth muscle actin (α-SMA). This procedure further enhances the effacement of the basement membrane, and increases in cell migration and invasion (7, 44).

The development of PF is associated with bioincompatible components in the dialysate containing HG, high osmolality, advanced glycation end products (AGE), uremic toxins, and so on. Numerous studies have stated that HG and glucose degradation products (GDP) promote transforming growth factor (TGF)-β and fibronectin production in the peritoneal mesothelial cells, which accelerates PF progression (17, 21, 24, 41).

TGF-β signaling has been described to play an essential role in tissue fibrosis (TF) (27, 36, 45). The TGF-β pathway was transduced via its downstream effector, the Smad proteins (9, 43). It can mediate the EMT process (23, 26, 30). Previous reports have shown that the TGF-β/Smad pathway is linked to the increases in α-SMA, collagen I, and (plasminogen activator inhibitor type 1) PAI-1 expression, which lead to the development of PF in rat animal models (29, 35). In addition, non-Smad signaling cascades such as phosphatidylinositol-3 kinase (PI3K)/Akt and Wnt/β-catenin/mammalian target of rapamycin (mTOR) signaling have been demonstrated to be involved in EMT (12, 19).

AMP-activated protein kinase (AMPK) is an important modulator of cellular energy or metabolic homeostasis (14, 38, 46). Recent reports have observed that AMPK activators [metformin or 5-aminoimidazole-4-carboxamide-1-β-D-ribofuranoside (AICAR)] have protective effects in experimental animals and humans (4, 5, 28, 33). The AMPK activator inhibits not only fibrosis (9, 22, 34) but also inflammation status (18, 31) and cancer (32, 37). In addition, AMPK activator ameliorated EMT (20).

HL156A is a novel AMPK activator synthesized by Hanall Biopharma. HL156A is a derivative of metformin synthesized in four steps from pyrrolidine (Fig. 1*A*). Preliminary in vitro cellular experiments exhibited that it elicits more potent AMPK activation than metformin or AICAR (Fig. 1*B*).

Therefore, in this study we investigated the protective mechanism of HL156A, a novel AMPK activator, against PF in in vivo and in vitro systems. The purposes of the present study are fourfold: *1*) Does HL156A inhibit the peritoneal fibrosis induced by chlorhexidine in a rat model? *2*) Is the AMPK activity of the mesothelial cell downregulated in the high glucose (HG) condition? *3*) What is the intracellular mechanism of action for the AMPK activator in the protection against PF? *4*) Is the antifibrotic effect of HL156A dependent on AMPK?

Address for reprint requests and other correspondence: K.-H. Oh, Dept. of Internal Medicine, Seoul National Univ. Hospital, 101 Daehak-ro, Chongno-Gu, Seoul, 03080, Seoul, Republic of Korea (e-mail: khoh@snu.ac.kr).

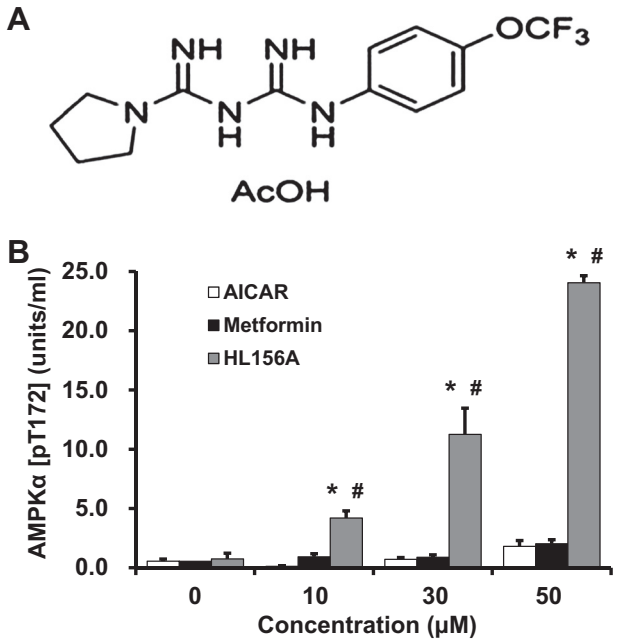

Fig. 1. Structure of HL156A and AMPK activity. *A*: structure of HL156A. *B*: AMPK activity of HL156A compared with other AMPK activators such as 5-aminoimidazole-4-carboxamide-1-β-D-ribofuranoside (AICAR) and metformin as determined by ELISA (Invitrogen, Carlsbad, CA). $*P < 0.05$ vs. AICAR. $\#P < 0.05$ vs. metformin.

MATERIALS AND METHODS

Synthesis of HL156A. The HL156A generation method is as follows. Concentrated hydrochloric acid was added to a solution prepared by dissolving pyrrolidine in butanol and stirred at 0°C for 30 min. Sodium dicyanamide was added to the mixed solution, and the resulting reaction mixture was stirred for 24 h under reflux. After completion of the reaction was confirmed, the adduct was purified. Concentrated hydrochloric acid was added to a solution obtained by dissolving the phenylamine in butanol and stirred at room temperature for 30 min. The N1-pyrollidine cyanoguanidine prepared above was added to the reaction mixture and stirred for 6 h under reflux. The reaction mixture was concentrated under reduced pressure, the concentrate was then dissolved while a 6 N hydrochloric acid/methanol solution was added, and ethyl acetate was added thereto. The formed solid was filtered, and the filter cake was dried under reduced pressure to obtain a white solid target compound, IM156A HCl. The IM156.HCl was converted to free form by adding sodium hydroxide The free form was converted to the acetate salt form by adding acetic acid providing IM156A.

Animals and treatments. Animal experiments were performed with the approval of the Institutional Animal Care and Use Committee (IACUC 12-0094) of Seoul National University Hospital. All rats had unrestricted access to food and water. Male Wistar rats (Koatech), weighing between 150 and 200 g, were divided into four groups (6 rats/group). PF was induced by daily intraperitoneal (ip) injection of 0.2 ml CHX solution including 0.1% CHX gluconate and 15% ethanol for 4 wk (16). Rats in the treatment group were supplemented ip daily with 1 mg/kg HL156A (Hanall Pharmaceuticals, Seoul, Korea), a novel AMPK activator. Control rats were injected with vehicle (D.W.) alone. Rats were maintained in compliance with IACUC protocols. At *week 4*, all rats were anesthetized, and the peritoneal tissues were dissected carefully. The peritoneum at the pole was embedded in paraffin for immunostaining or snap-frozen in liquid nitrogen (LN) to examine the protein expression levels.

Histological examination and immunohistochemistry. At the time of death, we defined encapsulating peritoneal sclerosis (EPS)-like changes as having more than two of the following five findings: bowel dilatation, peritoneal calcification, bowel adhesion, ascites with bleeding, and cocoon formation (Table 1). Fibronectin expression was measured by immunohistochemistry (IHC) with polyclonal antibodies or mouse monoclonal antibodies. For IHC, frozen sections (6-μm-thick) of paraformaldehyde (PFA)-fixed peritoneum were prepared. Before IHC, sections were pretreated with blocking solution consisting of 5% normal goat serum in PBS containing 0.1% BSA and 0.3% Triton X-100. Then, sections were incubated with the primary antibodies for 30 min in a humidified chamber at room temperature (RT). Thereafter, sections were washed three times in PBS-0.1% BSA and then incubated with a secondary anti-mouse IgG for 30 min at RT. The sections were then dehydrated and mounted with perrmount (Sigma, St. Louis, MO) and viewed by brightfield microscopy. The thickness of the peritoneum from each animal was determined in digital images using LAS imaging software (Leica Microsystems, Santa Barbara, CA).

Isolation and culture of primary rat peritoneal mesothelial cells. Rat peritoneal mesothelial cells (RPMCs) were isolated by using a trypsin digestion method as previously described and cultured (42). In brief, the whole anterior abdominal wall of male Wistar rats, weighing 150–200 g, were placed and fixed in an isolation device. The surface of parietal peritoneal cells was treated with prewarmed 0.25% trypsinase-EDTA-Na_2 for 30 min, and then a solution containing mesothelial cells was collected. The solution was centrifuged at 13,000 rpm for 10 min at RT. RPMCs were cultured in DMEM/F12 medium containing 15% (vol/vol) at 37°C in a humidified 5% CO_2 atmosphere. RPMCs from the third passage were used the following experiments. Primary cultured RPMCs were seeded in six-well plates or 10-cm^2 plastic culture dishes in DMEM/F12 medium under NG or HG conditions. When the primary RPMCs reached ~70–80% confluence, they were serum-starved for 24 h to synchronize cell growth. Afterward, the medium was replaced with completed media and treated with NG or HG in the presence or absence of 30 μM HL156A.

AMPK activity. AMPK activity in the RPMCs were assayed by ELISA kits (Invitrogen, Carlsbad, CA), according to the manufacturer's instruction.

RT-PCR. TGF-β1, fibronectin, AMPKα1/α2, Smad3, Snail, and mTOR gene expressions were assessed using RT-PCR. Total RNA was extracted from the RPMCs with TRIzol (Invitrogen Japan, Tokyo, Japan) by the guanidine thiocyanate extraction protocol. Total RNA was reverse transcribed into cDNA and then subjected to PCR using rat-specific primers. The primer sequences were as follows: TGF-β1, forward 5′-TGAGTGGCTGTCTTTTGACG-3′ and reverse 5′-TGGGACTGATCCCATTGATT-3′; AMPKα1, forward

Table 1. *Parameters of the experimental animals at euthanization*

	Body Weight, g	Glucose Level, mg/dl	BP, mmHg
Control ($n = 6$)	388.27 ± 12.04	105.67 ± 3.65	113.17 ± 0.95
Control+HL156A ($n = 6$)	376.22 ± 10.04	113.38 ± 4.27	114.26 ± 2.13
CHX ($n = 6$)	295.36 ± 5.34*	112.20 ± 4.08	111.78 ± 1.11
CHX+HL156A ($n = 6$)	326.49 ± 9.20	108.80 ± 2.65	110.07 ± 2.32

Values are means ± SE from 6 animals ($n = 6$) for each group. CHX, chlorohexidine; BP, blood pressure. $*P < 0.05$ vs. control.

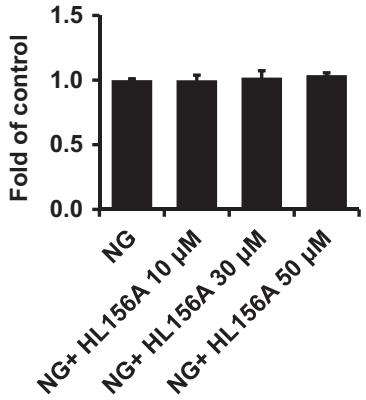

Fig. 2. Effects of HL156A supplement on cell toxicity in renal peritoneal mesothelial cells (RPMCs). Cell toxicity was detected by MTT assay for 24 h. RPMCs were cultured in normal-glucose (NG; 5 mM glucose) conditions supplemented with various concentrations of HL156A.

5′-ATCCGCAGAGAGATCCAGAA-3′ and reverse 5′-CGTCGACTCTCCTTTTCGTC-3′; AMPKα2, forward 5′-GCTGTGGATCGCCAAATTAT-3′ and reverse 5′-GCATCAGCAGAGTGGCAATA-3′; Smad3, forward 5′-CCTGGGCAAGTTCTCCAGAG-3′ and reverse 5′CCATCGCTGGCATCTTCTGTG-3′; Snail, forward 5′-GCTCCTTCCTGGTCAGGAAG-3′ and reverse 5′-GGCTGAGGTACTCCTTATTAC-3′; fibronectin, forward 5′-GTGGCTGCCTTCAACTTCTC-3′ and reverse 5′-AGTCCTTTAGGGCGG-3′; and GAPDH, forward 5′-ACCACAGTCCATGCCATCAC-3′ and reverse 5′-TCCACCACCCTGTTGCTGTA-3′.

Western blot analysis. The whole cell lysates (50 μg of protein/lane) were loaded, separated by 8–12% SDS- PAGE, and transferred onto nitrocellulose membranes (Amersham, Arlington Heights, IL). The membranes were blocked with 5% nonfat dry milk (skim milk) in Tris-buffered saline and 0.15% Tween 20 (TBS-T) for 2 h at RT. The proteins were detected by antibodies for TGF-β1 (sc-146), AMPKα (sc-25792), p-AMPKα (sc-33524), Snail (sc-10432), fibronectin (sc-9068; Santa Cruz Biotechnology, Santa Cruz, CA), Smad3 (9313), p-Smad3 (9520; Cell Signaling, Danvers, MA) diluted in TBS-T containing 5% dry milk and incubated overnight at 4°C in a between 1:500 and 1:1,000 dilution. After washing with TBS-T, the proteins were visualized using horseradish peroxidase-linked goat anti-mouse, goat anti-rabbit, or donkey anti-goat IgG (Santa Cruz Biotechnology) at 1:2,000 dilution, which was followed by ECL solution (Amersham). The chemiluminescent signals were captured on X-ray film.

Immunofluorescence staining and confocal microscopy. RPMCs cultured on coverslips were fixed with 4% PFA for 15 min at RT. After blocking with 1% BSA for 30 min, the slides were immunostained with primary antibodies for α-SMA (ab5694, Abcam, Cambridge, MA), p-Smad3 (9520, Cell Signaling), E-cadherin, (sc-8426), Snail (sc-10432), and fibronectin (sc-9068, Santa Cruz Biotechnology). Then, the slides were stained with a secondary antibody (Alexa) and mounted with mounting media (Dako, San Diego, CA) by using 4,6-diamidino-2-phenylindole to visualize the nuclei (Sigma). Slides were viewed under a Leica TSL-SL confocal microscope.

Small interfering RNA for AMPKα. RPMCs were seeded at a density of 1×10^5 cells/well on a six-well plate. RPMCs were grown to 70% confluence and serum-starved under NG conditions for 24 h. The specific AMPKα1 small interfering (si) RNA, AMPKα2 siRNA, or control siRNA (Santa Cruz Biotechnology) were transfected into the cells using a siRNA transfection reagent (Santa Cruz Biotechnology) according to the manufacturer's procedure. AMPKα1siRNA, AMPKα2 siRNA, or control siRNA were incubated at final concentration of 20 μM using siRNA dilution buffer (Santa Cruz Biotechnology) for 30 min at RT. The cells were washed twice with 2 ml of siRNA transfection medium (Santa Cruz Biotechnology), and 0.8 ml siRNA transfection medium and 200 μl siRNA transfection reagent complex were added to the well, covering the entire layer. The contents of the plate were gently mixed by swirling to ensure that the entire cell layer was immersed in the solution. Then, the cells were incubated for 5 h at 37°C in a 5% CO_2 incubator. After that, 1 ml of normal growth medium was added. Next, the cells were incubated for an additional 24 h. Then, the media were replaced with fresh completed media and treated with NG or HG in the presence or absence of HL156A for 24 h.

Statistical analysis. All values are expressed as the means ± SE. Statistical analyses were performed using the statistical package SPSS for Windows version 11.0 (SPSS, Chicago, IL). Results were analyzed using the Kruskal-Wallis nonparametric test for multiple comparisons. Significant differences by the Kruskal-Wallis test were confirmed by the Mann-Whitney *U*-test. P values <0.05 were considered statistically significant.

RESULTS

Toxicology assessments for HL156A. The maximal tolerability of the HL156A substance was evaluated in single doses and repeated doses in vivo. There were no meaningful toxicities with up to a 120 mg/kg dose (data not shown). We also investigated the toxicity of HL156A in RPMCs. RPMCs were cultured in NG conditions supplemented with various concentrations of HL156A (0, 10, 30, and 50 μM) for 24 h. The cell toxicity was detected by MTT assay for 24 h. There was no significant difference in cell toxicity among the various concentrations of HL156A (Fig. 2).

HL156A protects against PF induced by CHX. Our preliminary dose-finding experiment showed that 1 mg HL156A ameliorated PF most remarkably (Fig. 3). Intraperitoneal injection of a CHX solution for 4 wk showed peritoneal thickening with bowel adhesion, peritoneal calcification (Fig. 4*A*, white arrows), and cocoon formation (Fig. 4*A*, dashed circle). Such results were similar to the manifestations of human EPS cases (3, 15, 16, 39). Microscopically, CHX-treated rats exhibited a marked increase in peritoneal thickness (Fig. 4*B*) and fibronectin deposition in the peritoneal membrane (Fig. 4*C*).

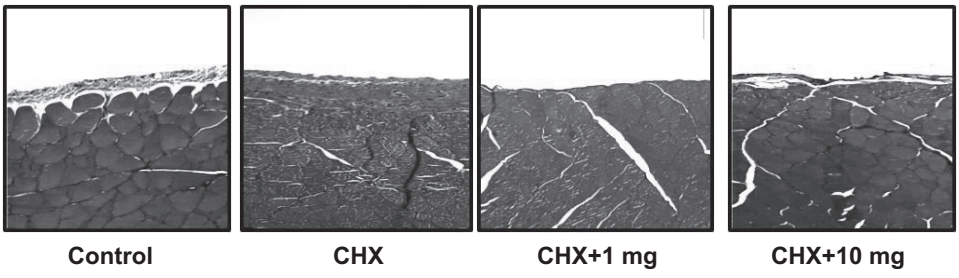

Fig. 3. Effects of HL156A supplement on chlorhexidine (CHX)-induced peritoneal thickness. To find the optimal dose of HL156A, we examined the thickness of peritoneal fibrosis using Masson's trichrome staining in rats treated with various doses of HL156A. CHX+1 mg, CHX+1 mg/kg HL156A; CHX+10 mg, CHX+10 mg/kg HL156A.

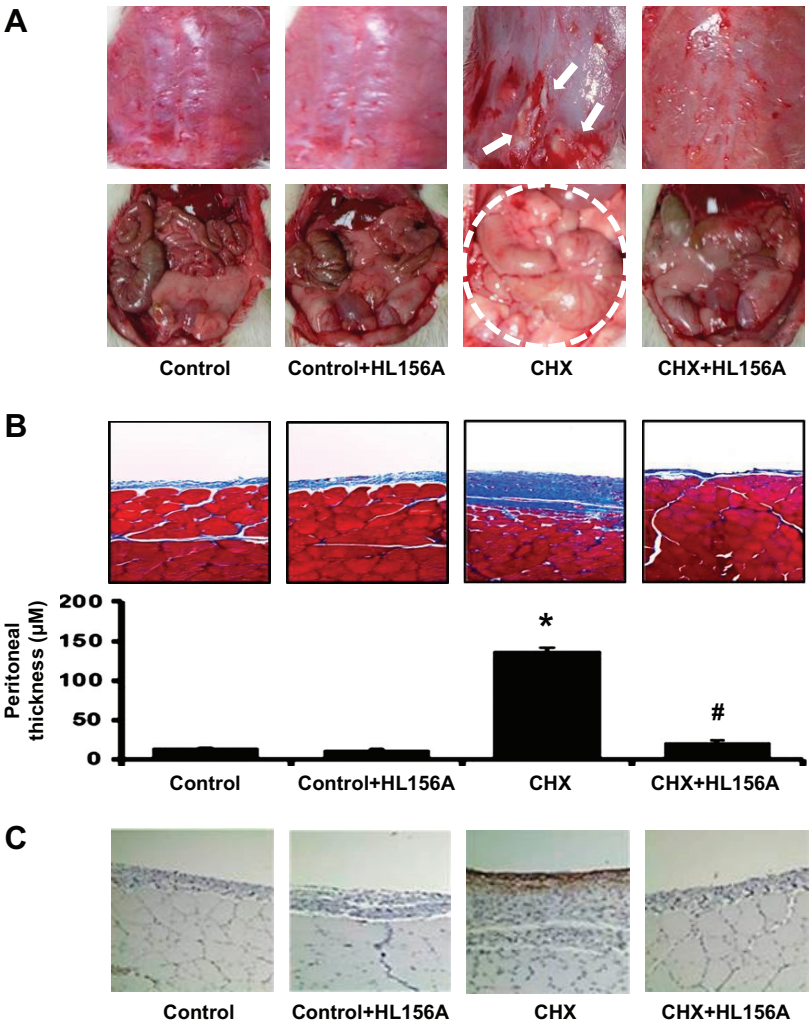

Fig. 4. Effects of HL156A treatment on peritoneal fibrosis. In the CHX-treated rats, severe inflammatory and fibrotic changes of the visceral peritoneum were evident, along with bowel obstruction, dilatation, calcification (white arrow), and cocoon formation (dashed circle). Treatment with HL156A (1 $mg \cdot kg^{-1} \cdot day^{-1}$) markedly ameliorated peritoneal damage (*A*). Thickness of the peritoneum was analyzed by the LAS imaging system. HL156A-treated rats showed reduced peritoneum thickness compared with the CHX group (*B*). The histograms represent means ± SE from 5 individual rats in each group. Representative micrographs show fibronectin immunostaining in the peritoneum (magnification: ×400; *C*) Control, D.W.-treated group; CHX, chlorhexidine-treated group; Control+HL156A, HL156A-supplemented D.W.-treated group; CHX+HL156A, HL156A-supplemented CHX-treated group. $*P < 0.05$ vs. control. $\#P < 0.05$ CHX+HL156A vs. CHX.

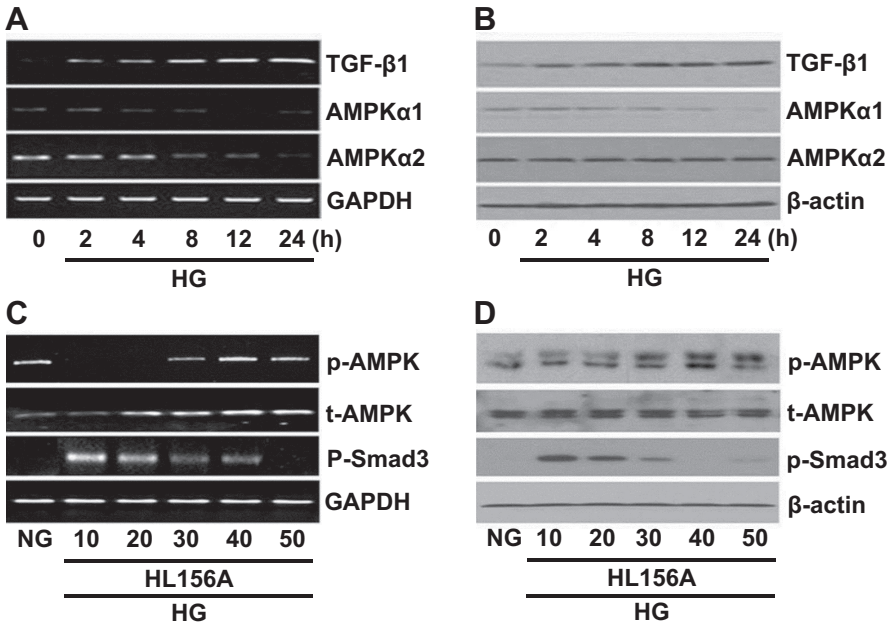

Fig. 5. mRNA and protein expression of high glucose (HG)-induced transforming growth factor (TGF)-β1 and AMPKα1/α2 in RPMCs. The cells were stimulated with HG (50 mM) for the designated time periods (*A* and *B*) or in HG (50 mM) supplemented with various concentration of HL156A (*C* and *D*).

However, such gross and histological changes were significantly ameliorated by HL156A treatment (Fig. 4, *A–C*). HL156A-treated rats showed a marked reduction in peritoneal thickness and fibronectin expression.

HL156A attenuated EMT induced by HG from RPMCs. RPMCs were cultured in NG- or HG-containing media. RPMCs exhibited a time-dependent increase in TGF-β and decrease in AMPKα1/α2 expression in the HG condition. Optimal treatment time with HG was 24 h (Fig. 5, *A* and *B*), and the concentration of HL156A was 30 μM (Fig. 5, *C* and *D*). RPMCs cultured in NG-containing media when confluent had a cobblestone-like appearance (Fig. 6*A*) with surface expression of E-cadherin and no expression of α-SMA (Fig. 6*B*). RPMCs cultured in HG-containing media transdifferentiated into a spindle-shaped appearance with a myofibroblast-like phenotype, indicative of EMT. However, such morphological changes in EMT were significantly attenuated by HL156A treatment (Fig. 6*A*). We confirmed the effect of HL156A on the expressions of α-SMA, p-Smad3, Snail, and fibronectin by using immunofluorescence analysis (Fig. 6*B*). Immunofluorescence data show that α-SMA, an EMT marker, was increased by HG. Also, Smad3, Snail, and fibronectin expression were also increased by treatment with HG (Fig. 6*B*). However, HG-induced fibrogenic markers were significantly attenuated by HL156A treatment (Fig. 6*B*). Therefore, HL156A treatment protects against EMT and ameliorated HG-stimulated upregulation of fibrogenic markers.

HG suppressed AMPKα expression and induced Smad3, Snail, and fibronectin expression in cultured RPMCs. RPMCs were cultured in HG conditions for 24 h. The mRNA and

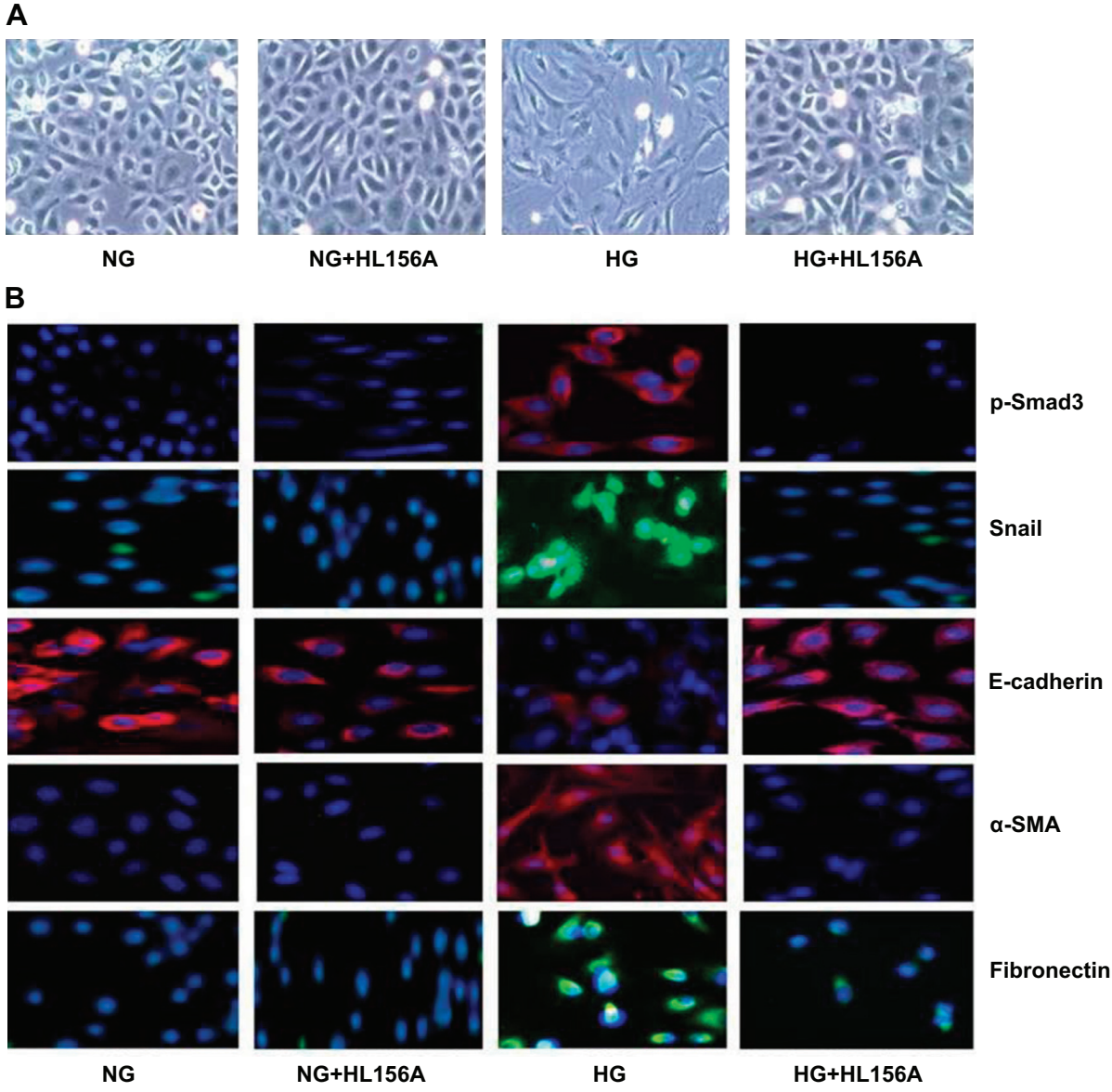

Fig. 6. Effects of HL156A on RPMC morphology. *A*: light microscopic appearance of representative RPMCs treated with NG or HG in the presence or absence of HL156A (30 μM). *B*: immunofluorescence staining shows expression of p-Smad3 (red), Snail (green), E-cadherin (red), α-SMA (red), and fibronectin (green). 4,6-Diamidino-2-phenylindole (DAPI; blue) is used for the nuclear marker. The cells were treated with or without HL156A (30 μM) and then stimulated with NG (5 mM) or HG (50 mM) for 24 h.

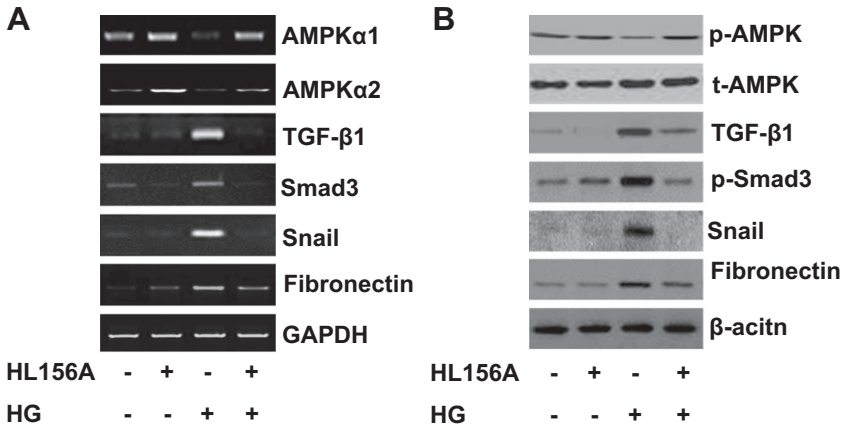

Fig. 7. Effects of HL156A treatment on mRNA and protein expression levels of AMPKα1/α2, TGF-β1, Smad3, Snail, and fibronectin in HG-stimulated RPMCs. The cells were treated with or without HL156A (30 μM) and then stimulated with NG (5 mM) or HG (50 mM) for 24 h.

protein expression levels of Smad3, Snail, and fibronectin were detected by RT-PCR and Western blot analysis. HG treatment induced expression of TGF-β1, a major fibrogenic growth factor. Smad3, Snail, and fibronectin increased in HG-treated RPMCs, and these increases were significantly attenuated by HL156A (30 μM) cotreatment (Fig. 7, *A* and *B*). These results suggest that HL156A treatment leads to significant suppression of Smad3, Snail, and fibronectin expression in the RPMCs, which had been upregulated in the HG condition.

HL156A recovered AMPKα1/α2 expression in RPMCs cultured in HG conditions. The effects of HL156A treatment on the mRNA and protein expression levels of AMPKα1/α2 were determined by RT-PCR and Western blot analysis. RPMCs cultured in HG conditions markedly decreased AMPKα1/α2 expression levels, which were recovered by HL156A cotreatment (Fig. 7, *A* and B). These results demonstrate that HL156A treatment leads to a significant upregulation of AMPKα1/α2 in the RPMCs, which was decreased in the HG condition. Effects of HL156A on the Smad3-dependent signaling of PF were also investigated. HL156A cotreatment also attenuated Smad3, Snail, and fibronectin, which were upregulated by HG treatment alone. Therefore, HL156A effectively suppressed Smad3-dependent pathways in the in vitro system.

Protective mechanism of HL156A on profibrotic signals is dependent on AMPKα1 in RPMCs. To identify the protective mechanism of HL156A in association with AMPK, we transiently knocked down the AMPK gene by transient siRNA in RPMCs. The knockdown effect of AMPK by AMPK α1 or AMPK α2 siRNA was confirmed by RT-PCR and Western blot analysis (Fig. 8). Since both AMPKα1 and AMPK α2 were upregulated by HL156A treatment (Fig. 7), the protective effects of HL156A in HG conditions were investigated by separately silencing AMPKα1 and AMPK α2 genes, respectively. Figure 9 shows knockdown of AMPK by AMPKα1 siRNA treatment abrogated the changes in Smad3, Snail, and fibronectin molecules, compared with the siRNA negative control. However, AMPKα2 siRNA did not change the mRNA and protein expressions of Smad3, Snail, and fibronectin molecules (Fig. 10). Taken together, silencing the AMPKα1 gene ameliorates the protective effect of HL156A, and the protective effect of HL156A in HG conditions is dependent on AMPKα1 upregulation.

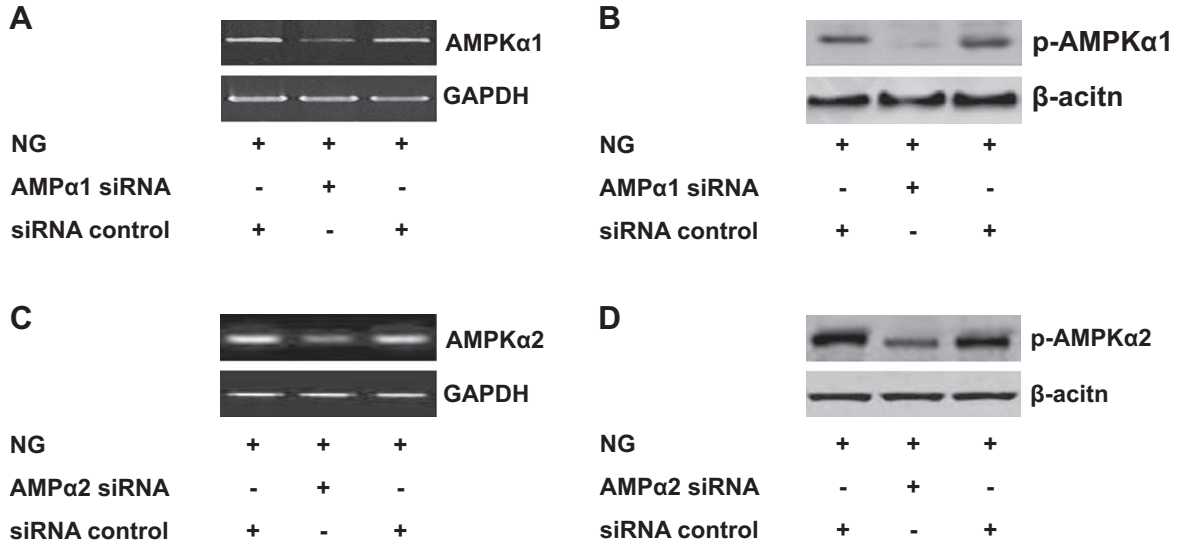

Fig. 8. Effects of knockdown of AMPK by AMPKα1/α2 small interfering RNA (siRNA). mRNA and protein expression levels of AMPKα1 and AMPKα2 by RT-PCR and Western blot analysis exhibited successful downregulation by AMPKα1 and AMPKα2 siRNA transfection to the RPMCs.

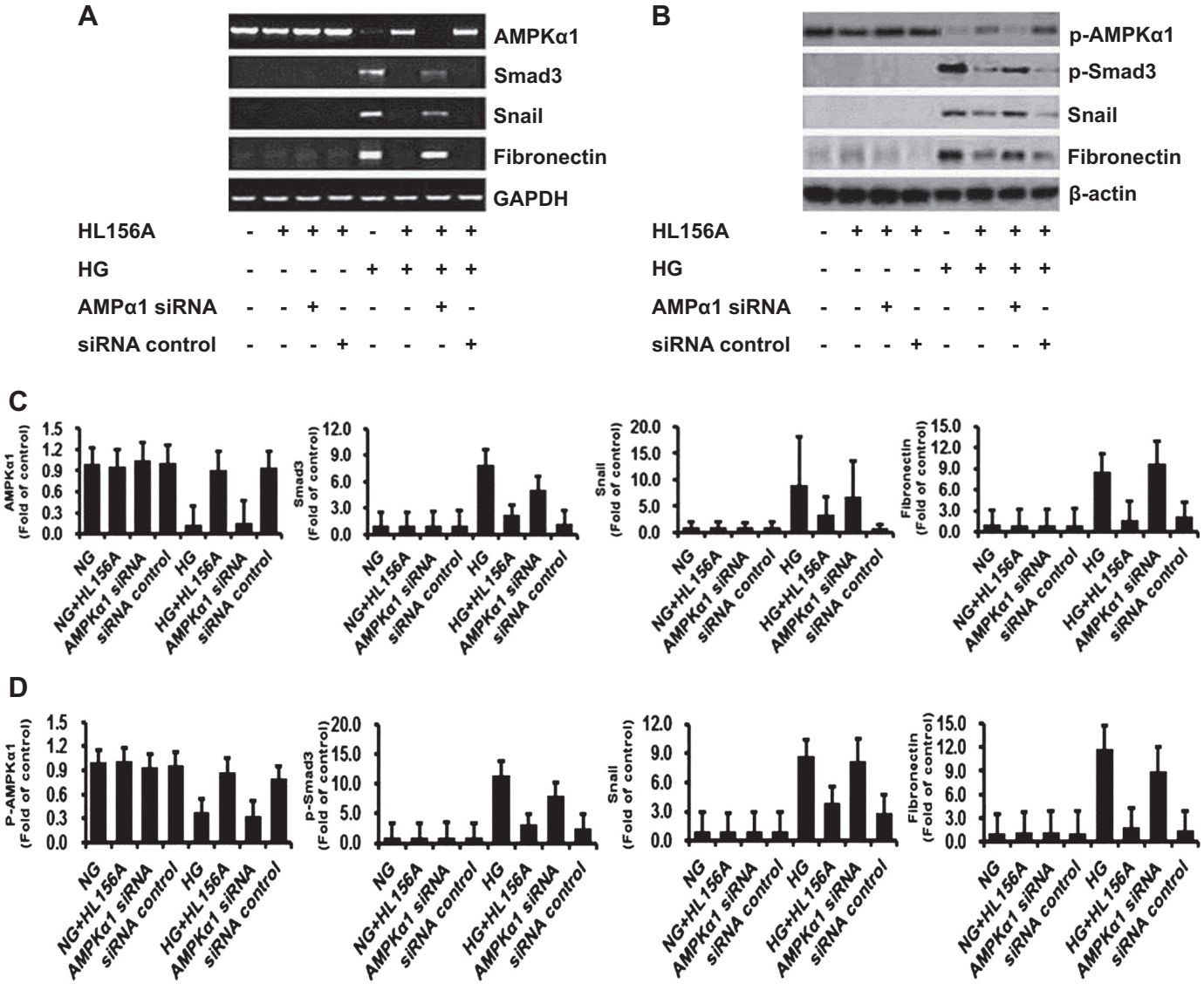

Fig. 9. Effects of AMPKα1 siRNA transfection to RPMCs on mRNA and protein expression levels of HG-induced Smad3, Snail, and fibronectin. The cells were transfected with AMPKα1 siRNA (20 μM) for 24 h. Then, the cells were stimulated with NG or HG in the presence or absence of HL156A (30 μM). mRNA and protein expression levels of Smad3, Snail, and fibronectin were determined by RT-PCR and Western blot analysis.

DISCUSSION

In the present study, we investigated the protective mechanism of HL156A, a novel AMPK activator, against the development and progression of PF in both in vivo and in vitro models. The major finding of our study is that the AMPK activator HL156A elicits a beneficial effect on the development and progression of PF. We showed that a HL156A supplement reduced peritoneal membrane thickness and expression of ECM molecules in a CHX-induced PF model. From in vitro experiments with RPMCs, we also showed that HL156A attenuated the morphological changes in RPMCs induced by HG conditions. HL156A increased AMPKα1/α2 expression, suppressed Smad3-dependent pathways activated by HG conditions, and downregulated various markers of EMT. Finally, we showed by gene-silencing studies that the antifibrotic effect of HL156A is an AMPKα-dependent mechanism.

Previous studies implicated that EMT is a crucial process of PF (11). Mesothelial cells, when exposed to HG, or GDP during peritoneal dialysis, secrete TGF-β, which is a potent profibrotic factor and induces EMT. Therefore, we examined TGF-β, α-SMA, E-cadherin, and Snail molecules previously implicated in EMT by HG conditions from RPMCs. Snail is well known to be a zinc finger regulator of gene expression which is modulated in EMT (10) and downregulates E-cadherin (6). We observed increased expression of p-Smad, Snail, and α-SMA and suppression of E-cadherin by HG. Previous study demonstrated that elevated Snail expression suppresses E-cadherin expression (44). Also, E-cadherin suppression and α-SMA upregulation are key processes in EMT which affect transformation and migration of epithelial cells (7). We have shown that HG-stimulated TGF-β1 upregulation, via p-Smad and Snail expression, inhibits E-cadherin expression and increases α-SMA. We have also shown that the above changes

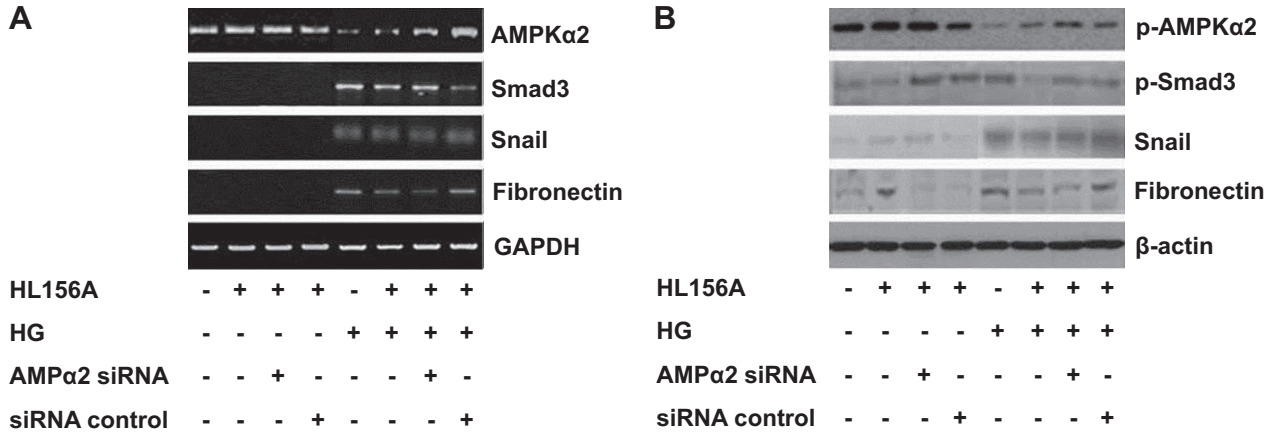

Fig. 10. Effects of AMPKα2 siRNA transfection on mRNA and protein expression levels of HG-induced Smad3, Snail, and fibronectin in RPMCs. The cells were transfected with AMPKα2 siRNA (20 μM) for 24 h. Then, the cells were stimulated with NG, or HG in the presence or absence of HL156A (30 μM).

induced by HG conditions are all abrogated by HL156A treatment.

AMPK upregulation seems to play a crucial role in the prevention of PF. AMPK upregulation by AMPK activators such as AICAR and metformin was recently reported to be protective in various fibrogenic conditions (4, 5, 9, 18, 20, 22, 28, 31–34, 37). HL156A is a novel and more potent activator of AMPK. AMPK forms a heterotrimer consisting of subunits α, β, and γ. Subunit α is the catalytic domain of AMPK. In the present study, since both the AMPKα1 and AMPKα2 were upregulated by HL156A treatment, we focused on which of the two AMPK isoforms is the main player in the antifibrotic mechanism of HL156A. Gene silencing of either AMPKα1 or AMPKα2 exhibited that knockdown only by AMPKα1 siRNA abrogated the protective effect of HL156A in RPMCs, but not by AMPKα2 siRNA. Therefore, the protective effect of HL156A is mediated by AMPK activation, which is mainly associated with AMPK α1.

In conclusion, the present study means that HL156A treatment protects against the development and progressions of experimental PF. The protective mechanism of HL156A is dependent on AMPK activation. The therapeutic potential of HL156A as an antifibrotic agent needs to be sought for in peritoneal dialysis patients.

GRANTS

This research was funded by Hanall Biopharma, Co. (Korea). However, the funding body had no role in the design, implementation, or interpretation of the study.

DISCLOSURES

No conflicts of interest, financial or otherwise, are declared by the authors.

AUTHOR CONTRIBUTIONS

Author contributions: K.D.J. and K.-H.O. provided conception and design of research; K.D.J. and J.L. performed experiments; K.D.J., B.T., E.J.C., Y.-H.H., J.Y., C.A., and K.-H.O. analyzed data; K.D.J., B.T., H.R., E.J.C., Y.-H.H., K.K., J.Y., C.A., and K.-H.O. interpreted results of experiments; K.D.J., H.J.K., B.T., H.R., and K.K. prepared figures; K.D.J., H.J.K., H.R., and J.Y. drafted manuscript; K.D.J., C.A., and K.-H.O. edited and revised manuscript; K.-H.O. approved final version of manuscript.

REFERENCES

1. **Aroeira LS, Aguilera A, Sanchez-Tomero JA, Bajo MA, del Peso G, Jimenez-Heffernan JA, Selgas R, Lopez-Cabrera M.** Epithelial to mesenchymal transition and peritoneal membrane failure in peritoneal dialysis patients: pathologic significance and potential therapeutic interventions. *J Am Soc Nephrol* 18: 2004–2013, 2007.
2. **Aroeira LS, Aguilera A, Selgas R, Ramirez-Huesca M, Perez-Lozano ML, Cirugeda A, Bajo MA, del Peso G, Sanchez-Tomero JA, Jimenez-Heffernan JA Lopez-Cabrera M.** Mesenchymal conversion of mesothelial cells as a mechanism responsible for high solute transport rate in peritoneal dialysis: role of vascular endothelial growth factor. *Am J Kidney Dis* 46: 938–948, 2005.
3. **Augustine T, Brown PW, Davies SD, Summers AM, Wilkie ME.** Encapsulating peritoneal sclerosis: clinical significance and implications. *Nephron Clin Pract* 111: c149–c154; discussion c154, 2009.
4. **Bergeron R, Previs SF, Cline GW, Perret P, Russell RR, 3rd Young LH, Shulman GI.** Effect of 5-aminoimidazole-4-carboxamide-1-beta-D-ribofuranoside infusion on in vivo glucose and lipid metabolism in lean and obese Zucker rats. *Diabetes* 50: 1076–1082, 2001.
5. **Bergheim I, Guo L, Davis MA, Lambert JC, Beier JI, Duveau I, Luyendyk JP, Roth RA, Arteel GE.** Metformin prevents alcohol-induced liver injury in the mouse: Critical role of plasminogen activator inhibitor-1. *Gastroenterology* 130: 2099–2112, 2006.
6. **Bolos V, Peinado H, Perez-Moreno MA, Fraga MF, Esteller M, Cano A.** The transcription factor Slug represses E-cadherin expression and induces epithelial to mesenchymal transitions: a comparison with Snail and E47 repressors. *J Cell Sci* 116: 499–511, 2003.
7. **Boyer B, Valles AM, Edme N.** Induction and regulation of epithelial-mesenchymal transitions. *Biochem Pharmacol* 60: 1091–1099, 2000.
8. **Brimble KS, Walker M, Margetts PJ, Kundhal KK, Rabbat CG.** Meta-analysis: peritoneal membrane transport, mortality, and technique failure in peritoneal dialysis. *J Am Soc Nephrol* 17: 2591–2598, 2006.
9. **Bujak M, Ren G, Kweon HJ, Dobaczewski M, Reddy A, Taffet G, Wang XF, Frangogiannis NG.** Essential role of Smad3 in infarct healing and in the pathogenesis of cardiac remodeling. *Circulation* 116: 2127–2138, 2007.
10. **Carver EA, Jiang R, Lan Y, Oram KF, Gridley T.** The mouse snail gene encodes a key regulator of the epithelial-mesenchymal transition. *Mol Cell Biol* 21: 8184–8188, 2001.
11. **Duan S, Yu J, Liu Q, Wang Y, Pan P, Xiao L, Ling G, Liu F.** Epithelial-to-mesenchymal transdifferentiation of peritoneal mesothelial cells mediated by oxidative stress in peritoneal fibrosis rats. *Zhong Nan Da Xue Xue Bao Yi Xue Ban* 36: 34–43, 2011.
12. **Fujishita T, Aoki K, Lane HA, Aoki M, Taketo MM.** Inhibition of the mTORC1 pathway suppresses intestinal polyp formation and reduces mortality in ApcDelta716 mice. *Proc Natl Acad Sci USA* 105: 13544–13549, 2008.
13. **Gokal R.** Peritoneal dialysis in the 21st century: an analysis of current problems and future developments. *J Am Soc Nephrol* 13, *Suppl* 1: S104–S116, 2002.
14. **Hardie DG.** AMPK: a key regulator of energy balance in the single cell and the whole organism. *Int J Obes (Lond)* 32, *Suppl* 4: S7–S12, 2008.
15. **Hirahara I, Ogawa Y, Kusano E, Asano Y.** Activation of matrix metalloproteinase-2 causes peritoneal injury during peritoneal dialysis in rats. *Nephrol Dial Transplant* 19: 1732–1741, 2004.

16. **Io H, Hamada C, Ro Y, Ito Y, Hirahara I, Tomino Y.** Morphologic changes of peritoneum and expression of VEGF in encapsulated peritoneal sclerosis rat models. *Kidney Int* 65: 1927–1936, 2004.
17. **Krediet RT, Lindholm B, Rippe B.** Pathophysiology of peritoneal membrane failure. *Perit Dial Int* 20, *Suppl* 4: S22–S42, 2000.
18. **Kubota S, Ozawa Y, Kurihara T, Sasaki M, Yuki K, Miyake S, Noda K, Ishida S, Tsubota K.** Roles of AMP-activated protein kinase in diabetes-induced retinal inflammation. *Invest Ophthalmol Vis Sci* 52: 9142–9148, 2011.
19. **Lamouille S, Derynck R.** Cell size and invasion in TGF-beta-induced epithelial to mesenchymal transition is regulated by activation of the mTOR pathway. *J Cell Biol* 178: 437–451, 2007.
20. **Lee JH, Kim JH, Kim JS, Chang JW, Kim SB, Park JS, Lee SK.** AMP-activated protein kinase inhibits TGF-beta-, angiotensin II-, aldosterone-, high glucose-, and albumin-induced epithelial-mesenchymal transition. *Am J Physiol Renal Physiol* 304: F686–F697, 2013.
21. **Leung JC, Chan LY, Tam KY, Tang SC, Lam MF, Cheng AS, Chu KM, Lai KN.** Regulation of CCN2/CTGF and related cytokines in cultured peritoneal cells under conditions simulating peritoneal dialysis. *Nephrol Dial Transplant* 24: 458–469, 2009.
22. **Lim JY, Oh MA, Kim WH, Sohn HY, Park SI.** AMP-activated protein kinase inhibits TGF-beta-induced fibrogenic responses of hepatic stellate cells by targeting transcriptional coactivator p300. *J Cell Physiol* 227: 1081–1089, 2012.
23. **Liu Y.** Epithelial to mesenchymal transition in renal fibrogenesis: pathologic significance, molecular mechanism, and therapeutic intervention. *J Am Soc Nephrol* 15: 1–12, 2004.
24. **Mandl-Weber S, Cohen CD, Haslinger B, Kretzler M, Sitter T.** Vascular endothelial growth factor production and regulation in human peritoneal mesothelial cells. *Kidney Int* 61: 570–578, 2002.
25. **Margetts PJ, Bonniaud P.** Basic mechanisms and clinical implications of peritoneal fibrosis. *Perit Dial Int* 23: 530–541, 2003.
26. **Margetts PJ, Bonniaud P, Liu L, Hoff CM, Holmes CJ, West-Mays JA, Kelly MM.** Transient overexpression of TGF-beta1 induces epithelial mesenchymal transition in the rodent peritoneum. *J Am Soc Nephrol* 16: 425–436, 2005.
27. **Miyazono K.** TGF-beta signaling by Smad proteins. *Cytokine Growth Factor Rev* 11: 15–22, 2000.
28. **Myerburg MM, King JD Jr, Oyster NM, Fitch AC, Magill A, Baty CJ, Watkins SC, Kolls JK, Pilewski JM, Hallows KR.** AMPK agonists ameliorate sodium and fluid transport and inflammation in cystic fibrosis airway epithelial cells. *Am J Respir Cell Mol Biol* 42: 676–684, 2010.
29. **Nie J, Dou X, Hao W, Wang X, Peng W, Jia Z, Chen W, Li X, Luo N, Lan HY, Yu XQ.** Smad7 gene transfer inhibits peritoneal fibrosis. *Kidney Int* 72: 1336–1344, 2007.
30. **Oh KH, Margetts PJ.** Cytokines and growth factors involved in peritoneal fibrosis of peritoneal dialysis patients. *Int J Artif Organs* 28: 129–134, 2005.
31. **Park SJ, Lee KS, Kim SR, Chae HJ, Yoo WH, Kim DI, Jeon MS, Lee YC.** AMPK activation reduces vascular permeability and airway inflammation by regulating HIF/VEGFA pathway in a murine model of toluene diisocyanate-induced asthma. *Inflamm Res* 61: 1069–1083, 2012.
32. **Sauer H, Engel S, Milosevic N, Sharifpanah F, Wartenberg M.** Activation of AMP-kinase by AICAR induces apoptosis of DU-145 prostate cancer cells through generation of reactive oxygen species and activation of c-Jun N-terminal kinase. *Int J Oncol* 40: 501–508, 2012.
33. **Shaw RJ, Lamia KA, Vasquez D, Koo SH, Bardeesy N, Depinho RA, Montminy M, Cantley LC.** The kinase LKB1 mediates glucose homeostasis in liver and therapeutic effects of metformin. *Science* 310: 1642–1646, 2005.
34. **Subramaniam N, Sherman MH, Rao R, Wilson C, Coulter S, Atkins AR, Evans RM, Liddle C, Downes M.** Metformin-mediated Bambi expression in hepatic stellate cells induces prosurvival Wnt/beta-catenin signaling. *Cancer Prev Res (Phila)* 5: 553–561, 2012.
35. **Sun Y, Zhu F, Yu X, Nie J, Huang F, Li X, Luo N, Lan HY, Wang Y.** Treatment of established peritoneal fibrosis by gene transfer of Smad7 in a rat model of peritoneal dialysis. *Am J Nephrol* 30: 84–94, 2009.
36. **Tahashi Y, Matsuzaki K, Date M, Yoshida K, Furukawa F, Sugano Y, Matsushita M, Himeno Y, Inagaki Y, Inoue K.** Differential regulation of TGF-beta signal in hepatic stellate cells between acute and chronic rat liver injury. *Hepatology* 35: 49–61, 2002.
37. **Vazquez-Martin A, Oliveras-Ferraros C, Cufi S, Del Barco S, Martin-Castillo B, Menendez JA.** Metformin regulates breast cancer stem cell ontogeny by transcriptional regulation of the epithelial-mesenchymal transition (EMT) status. *Cell Cycle* 9: 3807–3814, 2010.
38. **Viollet B, Guigas B, Sanz Garcia N, Leclerc J, Foretz M, Andreelli F.** Cellular and molecular mechanisms of metformin: an overview. *Clin Sci (Lond)* 122: 253–270, 2012.
39. **Washida N, Wakino S, Tonozuka Y, Homma K, Tokuyama H, Hara Y, Hasegawa K, Minakuchi H, Fujimura K, Hosoya K, Hayashi K, Itoh H.** Rho-kinase inhibition ameliorates peritoneal fibrosis and angiogenesis in a rat model of peritoneal sclerosis. *Nephrol Dial Transplant* 26: 2770–2779, 2011.
40. **Williams JD, Craig KJ, Topley N, Von Ruhland C, Fallon M, Newman GR, Mackenzie RK, Williams GT, and Peritoneal Biopsy Study Group.** Morphologic changes in the peritoneal membrane of patients with renal disease. *J Am Soc Nephrol* 13: 470–479, 2002.
41. **Witowski J, Korybalska K, Ksiazek K, Wisniewska-Elnur J, Jorres A, Lage C, Schaub TP, Passlick-Deetjen J, Breborowicz A, Grzegorzewska A, Ksiazek A, Liberek T, Lichodziejewska-Niemierko M, Majdan M, Rutkowski B, Stompor T, Sulowicz W.** Peritoneal dialysis with solutions low in glucose degradation products is associated with improved biocompatibility profile towards peritoneal mesothelial cells. *Nephrol Dial Transplant* 19: 917–924, 2004.
42. **Wu J, Yang X, Zhang YF, Zhou SF, Zhang R, Dong XQ, Fan JJ, Liu M, Yu XQ.** Angiotensin II upregulates Toll-like receptor 4 and enhances lipopolysaccharide-induced CD40 expression in rat peritoneal mesothelial cells. *Inflamm Res* 58: 473–482, 2009.
43. **Xiao H, Ma X, Feng W, Fu Y, Lu Z, Xu M, Shen Q, Zhu Y, Zhang Y.** Metformin attenuates cardiac fibrosis by inhibiting the TGFbeta1-Smad3 signalling pathway. *Cardiovasc Res* 87: 504–513, 2010.
44. **Yang J, Liu Y.** Dissection of key events in tubular epithelial to myofibroblast transition and its implications in renal interstitial fibrosis. *Am J Pathol* 159: 1465–1475, 2001.
45. **Zavadil J, Bottinger EP.** TGF-beta and epithelial-to-mesenchymal transitions. *Oncogene* 24: 5764–5774, 2005.
46. **Zhang BB, Zhou G, Li C.** AMPK: an emerging drug target for diabetes and the metabolic syndrome. *Cell Metab* 9: 407–416, 2009.